

A new {P₄Mo₆}-based complex as a highly efficient heterogeneous catalyst for the oxidation of alkylbenzenes under mild conditions

Xiaodong Liu, Na Xu, Xiaohui Liu, Yanyan Guo, Xiuli Wang*

College of Chemistry and Materials Engineering, Bohai University, Liaoning Professional Technology Innovation Center of Liaoning Province for Conversion Materials of Solar Cell, Jinzhou 121013, P. R. China

1. Materials and methods

All chemicals were purchased through commercial channels. All chemical materials were commercially purchased without further purification. Infrared (IR) spectra (KBr pellet) were performed on a Varian 640 IR infrared spectrophotometer in the range of 400-4000 cm⁻¹. Powder X-ray diffraction (PXRD) patterns were recorded on a D/teX Ultra diffractometer with Cu K α radiation ($\lambda = 1.5418 \text{ \AA}$). Simulated XRD data were simulated by the Mercury Software with the step of 0.02° from 5° to 50°. X-ray photoelectron spectrum (XPS) was measured using a Thermo Scientific K-Alpha photoelectron spectrometer. The catalytic reaction was analyzed by using a Shimadzu Tech-comp GC-7900 gas chromatograph (GC) with a flame ionization detector equipped with a TM-5 Sil capillary column. X-ray photoelectron spectrum (XPS) was measured using a Thermomo Scientific K-Alpha photoelectron spectrometer.

2. X-ray crystallographic study

The crystal data of the compounds were collected on a Bruker Apex CCD II area detector diffractometer with graphite-monochromated Mo K α radiation ($\lambda = 0.71073 \text{ \AA}$) at 273 K. Absorption corrections were applied using multiscan techniques. The structure was solved by direct methods and refined by full-matrix least-squares techniques using the SHELXL program¹⁻³. The contribution of disordered solvent molecules to the overall intensity data of structures was treated using the SQUEEZE method in PLATON. Crystallographic data for complex **1** is summarized in Table S1. The bond length (Å) and angle (deg) range, elected hydrogen bonding geometry of complex **1** is listed in Table S2-S4. BVS results compound **1** is listed in Table S5. The crystallographic data have been deposited with the Cambridge Crystallographic Data Centre (CCDC) as entries 2287157.

3. Selective oxidation of alkylbenzenes

The general method of selective oxidation of alkylbenzene is as follows: diphenylmethane, powdered catalyst (ball milling), solvent, and tert-butyl hydroperoxide (TBHP: 70% aqueous solution) were successively added to a 5 mL glass reaction tube to form a mixed solution. The mixed solution is then heated to the desired temperature in a parallel reactor. Naphthalene was used as an internal standard to analyze the product of the catalytic reaction. After the termination of the reaction, the catalyst was filtered and recovered, washed with acetonitrile, vacuum dried, and reused for the recyclability test.

4. Synthesis

Synthesis of $(\text{Hbz})_{10}\{\text{[Mn}_{1.5}(\mu_2-\text{O})_2(\text{H}_2\text{O})_2]\text{[Mn}(\text{H}_2\text{O})_3\}\{\text{Mn}[\text{Mo}_6\text{O}_{12}(\text{OH})_3(\text{H}_2\text{PO}_4)(\text{HPO}_4)_3]_2\}_2\cdot 4\text{H}_2\text{O}$ (**1**): The mixture of $\text{Na}_2\text{MoO}_4\cdot 2\text{H}_2\text{O}$ (0.50 g, 2.06 mmol), bz (0.118 g, 1 mmol), $\text{MnCl}_2\cdot 4\text{H}_2\text{O}$ (0.20 g, 1 mmol), H_3PO_4 (0.53 mL), 1 mL $\text{C}_2\text{H}_5\text{OH}$ and 5 mL H_2O was stirred for 0.5 h, and the pH of the mixed solution was adjusted to 1.4 with NaOH (1 M). The turbid liquid was sealed in a 25 mL Teflon-lined autoclave and heated at 160 °C for 4 days. After slow cooling to room temperature, dark red block crystals of complex **1** were achieved and filtered. Yield: ~ 0.305 g (61 % based on $\text{Na}_2\text{MoO}_4\cdot 2\text{H}_2\text{O}$). IR (KBr, cm^{-1}): 3144(w), 2981(m), 2883(m), 1620(s), 1535(w), 1501(w), 1451(s), 1407(w), 1388(w), 1234(m), 1153(w), 1065(w), 1007(w), 969(s), 932(s), 763(s), 736(w), 695(m), 603(m), 541(m), 500(m).

Synthesis of $\{\text{Mn}[\text{Mo}_6\text{O}_{12}(\text{OH})_3(\text{HPO}_4)_3(\text{PO}_4)]_2\}$ (**NENU-607**)⁴: An aqueous mixture of $\text{Na}_2\text{MoO}_4\cdot 2\text{H}_2\text{O}$ (0.33g, 1.38mmol), Mo powder (0.1g, 1.04mmol), H_3PO_3 (0.1g, 1.22mmol), $\text{MnCl}_2\cdot 4\text{H}_2\text{O}$ (0.1g, 0.50mmol), ethylenediamine (0.2 mL), $\text{H}_2\text{C}_2\text{O}_4$ (0.05g, 0.56mmol), DMF (1mL) and 6mL distilled water was stirred for 30 min, then the critical pH was adjusted to approximately 3.5 with H_3PO_4 (85%), then transfer it to a Teflon-lined reactor and kept temperature at 180 °C for 72 h. After 3 days, it was cooled down to room temperature at the rate of 10 °C / h. Eventually, red sheet crystals were obtained, washed by distilled water, and air-dried.

Synthesis of $[\text{Mn}(\text{P}_4\text{Mo}_6\text{O}_{32})]\cdot 5\text{H}_2\text{O}$ (**CUST-573**)⁵: Na_2MoO_4 (0.24 g, 1 mmol), 1,4-bis[(1H-imidazole-1-yl) methyl]benzene (0.024 g, 0.1 mmol), $\text{MnCl}_2\cdot 4\text{H}_2\text{O}$ (0.059 g, 0.3 mmol), H_3PO_4 (1.00 mL), H_2O (5.0 mL, 0.275 mol) and CH_3OH (1 mL) were mixed and stirred for 30 min. NaOH was added to adjust pH to 2.0. The mixture was then transferred to a teflon-lined reactor and kept at 180 °C for 3 days. After the reactor was cooled to room temperature at a rate of 10 °C / h, red block crystals were obtained, which were washed with distilled water and air-dried.

Table S1. Crystal data and structure refinement for complex **1**.

Complex 1	
Empirical formula	C ₇₀ H ₁₁₈ Mn ₇ Mo ₂₄ N ₂₀ O ₁₄₂ P ₁₆
CCDC code	2287157
Formula weight	6694.50
Crystal system	Triclinic
Space group	<i>P</i> 1
<i>T</i> (K)	273
<i>a</i> (Å)	14.7317(13)
<i>b</i> (Å)	15.1925(14)
<i>c</i> (Å)	20.7026(19)
α (°)	97.426(2)
β (°)	105.699(2)
γ (°)	93.850(2)
<i>V</i> (Å ³)	4397.0(7)
<i>Z</i>	1
D _c (Mg m ⁻³)	2.528
μ (mm ⁻¹)	2.401
<i>F</i> (000)	3201.17
Reflections collected / unique	24984 / 15287 [R(int) = 0.0158]
Data/ restraints / parameters	15287 / 286 / 1330
GOF	1.069
R index [<i>I</i> > 2σ(<i>I</i>)]	R ₁ = 0.0396, wR ₂ = 0.0946
R (all data)	R ₁ = 0.0452, wR ₂ = 0.0979

$$R_1 = \sum |F_o| - |F_c| / \sum |F_o|; wR_2 = \{\sum [w(F_o^2 - F_c^2)^2] / \sum [w(F_o^2)^2]\}^{1/2}$$

Table S2. The selected bond length (Å) in complex **1**.

Bond	Length (Å)	Bond	Length (Å)	Bond	Length (Å)	Bond	Length (Å)
Mo(1)-Mo(11)	2.5900(7)	Mo(5)-O(14)	1.976(4)	Mo(9)-O(6)	1.984(4)	Mn(1)-O(69A)	2.191(18)
Mo(1)-O(1)	2.126(4)	Mo(5)-O(26)	2.113(4)	Mo(9)-O(36)	2.270(4)	Mn(1)-O(2A)	2.127(19)
Mo(1)-O(10)	1.980(4)	Mo(5)-O(54)	1.932(4)	Mo(9)-O(44)	1.924(4)	Mn(1)-O(9)	2.259(6)
Mo(1)-O(34)	2.053(4)	Mo(5)-O(56)	2.340(4)	Mo(9)-O(52)	2.046(4)	Mn(2)-O(46)	2.141(4)
Mo(1)-O(36)	2.277(4)	Mo(5)-O(7)	2.037(4)	Mo(9)-O(47)	1.680(4)	Mn(2)-O(55)#2	2.189(5)
Mo(1)-O(42)	1.941(4)	Mo(5)-O(29)	1.669(5)	Mo(10)-Mo(3)	2.5932(7)	Mn(2)-O(59)	2.231(5)
Mo(1)-O(66)	1.673(4)	Mo(6)-Mo(2)	2.5983(7)	Mo(10)-O(4)	2.104(4)	Mn(2)-O(63)	2.176(5)
Mo(2)-O(8)	1.982(4)	Mo(6)-O(8)	1.978(4)	Mo(10)-O(22)	2.283(4)	Mn(2)-O(2)	2.234(9)
Mo(2)-O(20)	2.112(4)	Mo(6)-O(18)	2.091(4)	Mo(10)-O(24)	1.974(4)	Mn(2)-O(67)	2.219(9)
Mo(2)-O(28)	2.298(4)	Mo(6)-O(30)	2.309(4)	Mo(10)-O(32)	1.940(4)	Mn(3)-O(46)	2.166(5)
Mo(2)-O(64)	1.954(4)	Mo(6)-O(64)	1.952(4)	Mo(10)-O(58)	2.072(4)	Mn(3)-O(59)	2.094(5)
Mo(2)-O(5)	2.068(4)	Mo(6)-O(43)	2.056(4)	Mo(10)-O(3)	1.675(4)	Mn(3)-O(31)	1.991(5)
Mo(2)-O(25)	1.671(4)	Mo(6)-O(13)	1.664(4)	Mo(11)-O(10)	1.969(4)	Mn(3)-O(33)	2.181(10)
Mo(2)-O(8)	1.982(4)	Mo(7)-O(12)	1.964(4)	Mo(11)-O(26)	2.114(4)	Mn(3)-O(69A)	1.709(17)
Mo(3)-O(20)	2.115(4)	Mo(7)-O(18)	2.094(4)	Mo(11)-O(42)	1.938(4)	Mn(4)-O(38)	2.133(4)
Mo(3)-O(24)	1.967(4)	Mo(7)-O(30)	2.265(4)	Mo(11)-O(48)	2.089(4)	Mn(4)-O(37)	2.200(4)
Mo(3)-O(28)	2.233(4)	Mo(7)-O(50)	2.069(4)	Mo(11)-O(56)	2.256(4)	Mn(4)-O(39)	2.204(5)
Mo(3)-O(32)	1.939(4)	Mo(7)-O(70)	1.940(4)	Mo(11)-O(62)	1.675(4)	Mn(4)-O(53)	2.244(5)
Mo(3)-O(60)	2.091(4)	Mo(7)-O(49)	1.678(4)	Mo(12)-Mo(7)	2.5891(7)	Mn(4)-O(15)	2.229(5)
Mo(3)-O(21)	1.675(4)	Mo(8)-Mo(5)	2.5949(8)	Mo(12)-O(4)	2.118(4)	Mn(4)-O(65)	2.292(6)

Mo(4)-Mo(9)	2.5944(7)	Mo(8)-O(14)	1.982(4)	Mo(12)-O(12)	1.982(4)	Mn(5)-O(6)#1	2.186(4)
Mo(4)-O(6)	1.969(4)	Mo(8)-O(16)	2.090(4)	Mo(12)-O(22)	2.292(4)	Mn(5)-O(8)	2.198(4)
Mo(4)-O(16)	2.086(4)	Mo(8)-O(40)	2.309(4)	Mo(12)-O(70)	1.936(4)	Mn(5)-O(10)#1	2.203(4)
Mo(4)-O(40)	2.265(4)	Mo(8)-O(54)	1.936(4)	Mo(12)-O(11)	1.676(4)	Mn(5)-O(12)	2.189(4)
Mo(4)-O(44)	1.941(4)	Mo(8)-O(68)	2.056(4)	Mo(12)-O(23)	2.034(4)	Mn(5)-O(14)#1	2.201(4)
Mo(4)-O(71)	2.088(4)	Mo(8)-O(45)	1.667(5)	Mn(1)-O(46)	2.141(6)	Mn(5)-O(24)	2.202(4)
Mo(4)-O(19)	1.674(4)	Mo(9)-O(1)	2.146(4)	Mn(1)-O(59)	2.120(6)		

Symmetry code: #1, x+1, y, z; #2, -x+1, -y+1, -z.

Table S3. The selected bond angle (deg) in complex 1.

Bond	Angle (°)	Bond	Angle (°)	Bond	Angle (°)
O(1)-Mo(1)-Mo(11)	133.37(11)	O(64)-Mo(6)-O(8)	95.80(17)	O(62)-Mo(11)-O(10)	103.42(19)
O(1)-Mo(1)-O(36)	72.05(14)	O(64)-Mo(6)-O(18)	154.83(17)	O(62)-Mo(11)-O(26)	95.25(19)
O(10)-Mo(1)-Mo(11)	48.82(11)	O(64)-Mo(6)-O(30)	83.31(16)	O(62)-Mo(11)-O(42)	105.5(2)
O(10)-Mo(1)-O(1)	85.85(16)	O(64)-Mo(6)-O(43)	86.45(18)	O(62)-Mo(11)-O(48)	93.2(2)
O(10)-Mo(1)-O(34)	160.95(17)	O(43)-Mo(6)-Mo(2)	134.47(13)	O(62)-Mo(11)-O(56)	167.35(19)
O(10)-Mo(1)-O(36)	79.49(15)	O(43)-Mo(6)-O(18)	83.37(17)	O(4)-Mo(12)-Mo(7)	132.84(11)
O(34)-Mo(1)-Mo(11)	136.76(12)	O(43)-Mo(6)-O(30)	79.63(16)	O(4)-Mo(12)-O(22)	72.64(15)
O(34)-Mo(1)-O(1)	82.53(16)	O(13)-Mo(6)-Mo(2)	100.60(17)	O(12)-Mo(12)-Mo(7)	48.68(11)
O(34)-Mo(1)-O(36)	82.58(16)	O(13)-Mo(6)-O(8)	101.0(2)	O(12)-Mo(12)-O(4)	85.27(16)
O(36)-Mo(1)-Mo(11)	87.23(10)	O(13)-Mo(6)-O(18)	97.6(2)	O(12)-Mo(12)-O(22)	80.25(15)
O(42)-Mo(1)-Mo(11)	48.07(12)	O(13)-Mo(6)-O(30)	169.56(19)	O(12)-Mo(12)-O(23)	159.80(17)

O(42)-Mo(1)-O(1)	154.81(17)	O(13)-Mo(6)-O(64)	106.5(2)	O(22)-Mo(12)-Mo(7)	87.80(10)
O(42)-Mo(1)-O(10)	95.31(17)	O(13)-Mo(6)-O(43)	97.1(2)	O(70)-Mo(12)-Mo(7)	48.17(13)
O(42)-Mo(1)-O(34)	88.95(17)	O(12)-Mo(7)-Mo(12)	49.30(12)	O(70)-Mo(12)-O(4)	156.43(17)
O(42)-Mo(1)-O(36)	83.40(16)	O(12)-Mo(7)-O(18)	87.12(16)	O(70)-Mo(12)-O(12)	95.47(17)
O(66)-Mo(1)-Mo(11)	100.84(15)	O(12)-Mo(7)-O(30)	82.30(15)	O(70)-Mo(12)-O(22)	84.24(16)
O(66)-Mo(1)-O(1)	98.29(19)	O(12)-Mo(7)-O(50)	160.86(17)	O(70)-Mo(12)-O(23)	86.00(18)
O(66)-Mo(1)-O(10)	101.61(19)	O(18)-Mo(7)-Mo(12)	135.47(12)	O(11)-Mo(12)-Mo(7)	101.12(15)
O(66)-Mo(1)-O(34)	95.0(2)	O(18)-Mo(7)-O(30)	73.11(15)	O(11)-Mo(12)-O(4)	97.11(19)
O(66)-Mo(1)-O(36)	170.23(18)	O(30)-Mo(7)-Mo(12)	89.95(10)	O(11)-Mo(12)-O(12)	101.43(19)
O(66)-Mo(1)-O(42)	106.1(2)	O(50)-Mo(7)-Mo(12)	133.05(12)	O(11)-Mo(12)-O(22)	169.52(19)
O(8)-Mo(2)-Mo(6)	48.93(12)	O(50)-Mo(7)-O(18)	84.61(17)	O(11)-Mo(12)-O(70)	105.8(2)
O(8)-Mo(2)-O(20)	85.34(16)	O(50)-Mo(7)-O(30)	78.80(15)	O(11)-Mo(12)-O(23)	97.5(2)
O(8)-Mo(2)-O(28)	80.62(15)	O(70)-Mo(7)-Mo(12)	48.02(12)	O(23)-Mo(12)-Mo(7)	133.64(14)
O(8)-Mo(2)-O(5)	160.13(17)	O(70)-Mo(7)-O(12)	95.93(17)	O(23)-Mo(12)-O(4)	85.50(17)
O(20)-Mo(2)-Mo(6)	133.28(11)	O(70)-Mo(7)-O(18)	157.33(17)	O(23)-Mo(12)-O(22)	79.86(17)
O(20)-Mo(2)-O(28)	72.44(15)	O(70)-Mo(7)-O(30)	85.01(16)	O(46)-Mn(1)-O(9)	107.8(2)
O(28)-Mo(2)-Mo(6)	88.78(10)	O(70)-Mo(7)-O(50)	85.40(17)	O(46)-Mn(1)-O(2)	76.9(3)
O(64)-Mo(2)-Mo(6)	48.28(12)	O(49)-Mo(7)-Mo(12)	101.87(15)	O(46)-Mn(1)-H(2A)	81
O(64)-Mo(2)-O(8)	95.59(17)	O(49)-Mo(7)-O(12)	102.08(19)	O(46)-Mn(1)-O(69A)	89.8(5)
O(64)-Mo(2)-O(20)	156.14(17)	O(49)-Mo(7)-O(18)	95.18(19)	O(46)-Mn(1)-H(69D)	89.5
O(64)-Mo(2)-O(28)	84.16(16)	O(49)-Mo(7)-O(30)	167.43(19)	O(9)-Mn(1)-O(2)	73.9(3)
O(64)-Mo(2)-O(5)	85.62(18)	O(49)-Mo(7)-O(50)	95.84(19)	O(9)-Mn(1)-H(2A)	56.6

O(5)-Mo(2)-Mo(6)	133.55(14)	O(49)-Mo(7)-O(70)	106.0(2)	O(9)-Mn(1)-H(69D)	71.2
O(5)-Mo(2)-O(20)	85.70(17)	O(14)-Mo(8)-Mo(5)	48.93(11)	O(59)-Mn(1)-O(46)	79.5(2)
O(5)-Mo(2)-O(28)	79.78(16)	O(14)-Mo(8)-O(16)	86.34(16)	O(59)-Mn(1)-O(9)	167.2(3)
O(25)-Mo(2)-Mo(6)	100.35(17)	O(14)-Mo(8)-O(40)	79.94(15)	O(59)-Mn(1)-O(2)	98.2(3)
O(25)-Mo(2)-O(8)	101.6(2)	O(14)-Mo(8)-O(68)	159.40(17)	O(59)-Mn(1)-H(2A)	115.9
O(25)-Mo(2)-O(20)	97.5(2)	O(16)-Mo(8)-Mo(5)	134.27(12)	O(59)-Mn(1)-O(69A)	97.6(5)
O(25)-Mo(2)-O(28)	169.6(2)	O(16)-Mo(8)-O(40)	71.85(15)	O(59)-Mn(1)-H(69D)	120.1
O(25)-Mo(2)-O(64)	105.6(2)	O(40)-Mo(8)-Mo(5)	88.91(10)	O(59)-Mn(1)-O(2A)	90.5(6)
O(25)-Mo(2)-O(5)	97.1(2)	O(54)-Mo(8)-Mo(5)	47.81(13)	O(2)-Mn(1)-H(2A)	17.7
O(20)-Mo(3)-Mo(10)	134.53(11)	O(54)-Mo(8)-O(14)	94.95(17)	O(69)-Mn(1)-O(46)	109.7(4)
O(20)-Mo(3)-O(28)	73.72(15)	O(54)-Mo(8)-O(16)	155.44(18)	O(69)-Mn(1)-O(9)	80.4(3)
O(24)-Mo(3)-Mo(10)	48.98(11)	O(54)-Mo(8)-O(40)	84.20(17)	O(69)-Mn(1)-O(59)	107.5(3)
O(24)-Mo(3)-O(20)	86.32(16)	O(54)-Mo(8)-O(68)	86.92(18)	O(69)-Mn(1)-O(2A)	156.8(6)
O(24)-Mo(3)-O(28)	82.33(15)	O(68)-Mo(8)-Mo(5)	134.39(13)	O(69A)-Mn(1)-O(9)	93.0(5)
O(24)-Mo(3)-O(60)	162.03(17)	O(68)-Mo(8)-O(16)	83.66(17)	O(69A)-Mn(1)-H(69D)	23
O(28)-Mo(3)-Mo(10)	90.10(10)	O(68)-Mo(8)-O(40)	79.84(16)	O(2A)-Mn(1)-O(46)	87.5(6)
O(32)-Mo(3)-Mo(10)	48.08(12)	O(45)-Mo(8)-Mo(5)	99.87(16)	O(2A)-Mn(1)-O(9)	79.6(5)
O(32)-Mo(3)-O(20)	158.55(17)	O(45)-Mo(8)-O(14)	100.9(2)	O(46)-Mn(2)-O(55)#2	161.19(19)
O(32)-Mo(3)-O(24)	95.70(16)	O(45)-Mo(8)-O(16)	97.3(2)	O(46)-Mn(2)-O(59)	77.10(17)
O(32)-Mo(3)-O(28)	85.35(16)	O(45)-Mo(8)-O(40)	169.09(19)	O(46)-Mn(2)-O(63)	109.76(18)
O(32)-Mo(3)-O(60)	86.41(17)	O(45)-Mo(8)-O(54)	106.5(2)	O(46)-Mn(2)-O(2)	82.7(3)
O(60)-Mo(3)-Mo(10)	134.22(13)	O(45)-Mo(8)-O(68)	98.2(2)	O(46)-Mn(2)-O(67)	84.8(2)

O(60)-Mo(3)-O(20)	85.38(16)	O(1)-Mo(9)-Mo(4)	132.65(11)	O(55)#2-Mn(2)-O(59)	90.11(18)
O(60)-Mo(3)-O(28)	80.05(16)	O(1)-Mo(9)-O(36)	71.83(15)	O(55)#2-Mn(2)-O(2)	86.9(3)
O(21)-Mo(3)-Mo(10)	102.14(16)	O(6)-Mo(9)-Mo(4)	48.72(11)	O(55)#2-Mn(2)-O(67)	107.7(2)
O(21)-Mo(3)-O(20)	94.7(2)	O(6)-Mo(9)-O(1)	85.13(16)	O(59)-Mn(2)-O(2)	103.1(4)
O(21)-Mo(3)-O(24)	102.76(19)	O(6)-Mo(9)-O(36)	79.41(15)	O(63)-Mn(2)-O(55)#2	86.23(18)
O(21)-Mo(3)-O(28)	167.18(19)	O(6)-Mo(9)-O(52)	159.10(16)	O(63)-Mn(2)-O(59)	163.9(2)
O(21)-Mo(3)-O(32)	105.6(2)	O(36)-Mo(9)-Mo(4)	87.47(10)	O(63)-Mn(2)-O(2)	92.4(4)
O(21)-Mo(3)-O(60)	93.8(2)	O(44)-Mo(9)-Mo(4)	48.11(13)	O(63)-Mn(2)-O(67)	82.3(2)
O(6)-Mo(4)-Mo(9)	49.24(11)	O(44)-Mo(9)-O(1)	155.61(17)	O(67)-Mn(2)-O(59)	83.9(2)
O(6)-Mo(4)-O(16)	87.29(16)	O(44)-Mo(9)-O(6)	95.37(17)	O(67)-Mn(2)-O(2)	164.0(4)
O(6)-Mo(4)-O(40)	82.57(15)	O(44)-Mo(9)-O(36)	84.25(16)	O(46)-Mn(3)-O(33)	171.7(3)
O(6)-Mo(4)-O(71)	161.00(16)	O(44)-Mo(9)-O(52)	86.19(18)	O(46)-Mn(3)-O(69)	97.3(3)
O(16)-Mo(4)-Mo(9)	135.51(12)	O(52)-Mo(9)-Mo(4)	133.74(13)	O(46)-Mn(3)-H(69A)	108
O(16)-Mo(4)-O(40)	72.82(15)	O(52)-Mo(9)-O(1)	85.02(17)	O(59)-Mn(3)-O(46)	79.53(17)
O(16)-Mo(4)-O(71)	84.37(17)	O(52)-Mo(9)-O(36)	80.01(16)	O(59)-Mn(3)-O(33)	107.6(3)
O(40)-Mo(4)-Mo(9)	90.12(10)	O(47)-Mo(9)-Mo(4)	101.96(16)	O(59)-Mn(3)-O(69)	96.9(3)
O(44)-Mo(4)-Mo(9)	47.56(12)	O(47)-Mo(9)-O(1)	96.80(19)	O(59)-Mn(3)-H(69A)	117.2
O(44)-Mo(4)-O(6)	95.34(17)	O(47)-Mo(9)-O(6)	101.79(19)	O(31)-Mn(3)-O(46)	91.72(19)
O(44)-Mo(4)-O(16)	156.77(17)	O(47)-Mo(9)-O(36)	168.50(19)	O(31)-Mn(3)-O(59)	112.2(2)
O(44)-Mo(4)-O(40)	84.62(16)	O(47)-Mo(9)-O(44)	106.9(2)	O(31)-Mn(3)-O(33)	81.8(3)
O(44)-Mo(4)-O(71)	85.90(17)	O(47)-Mo(9)-O(52)	97.7(2)	O(31)-Mn(3)-O(69)	150.6(3)
O(71)-Mo(4)-Mo(9)	133.16(12)	O(4)-Mo(10)-Mo(3)	133.29(11)	O(31)-Mn(3)-H(69A)	129.1

O(71)-Mo(4)-O(40)	78.67(15)	O(4)-Mo(10)-O(22)	73.06(15)	O(69)-Mn(3)-H(69A)	21.9
O(19)-Mo(4)-Mo(9)	101.63(15)	O(22)-Mo(10)-Mo(3)	87.29(10)	O(69A)-Mn(3)-O(46)	103.7(6)
O(19)-Mo(4)-O(6)	101.87(19)	O(24)-Mo(10)-Mo(3)	48.74(11)	O(69A)-Mn(3)-O(59)	116.7(6)
O(19)-Mo(4)-O(16)	95.60(19)	O(24)-Mo(10)-O(4)	85.83(16)	O(69A)-Mn(3)-O(31)	130.5(6)
O(19)-Mo(4)-O(40)	167.53(18)	O(24)-Mo(10)-O(22)	80.70(15)	O(69A)-Mn(3)-O(33)	77.1(6)
O(19)-Mo(4)-O(44)	106.4(2)	O(24)-Mo(10)-O(58)	160.99(17)	O(38)-Mn(4)-O(37)	91.36(17)
O(19)-Mo(4)-O(71)	95.92(19)	O(32)-Mo(10)-Mo(3)	48.04(12)	O(38)-Mn(4)-O(39)	112.29(16)
O(14)-Mo(5)-Mo(8)	49.13(11)	O(32)-Mo(10)-O(4)	155.80(17)	O(38)-Mn(4)-O(53)	84.73(18)
O(14)-Mo(5)-O(26)	85.46(16)	O(32)-Mo(10)-O(22)	83.27(16)	O(38)-Mn(4)-O(15)	85.85(19)
O(14)-Mo(5)-O(56)	80.25(15)	O(32)-Mo(10)-O(24)	95.43(17)	O(38)-Mn(4)-O(65)	163.6(2)
O(14)-Mo(5)-O(7)	159.46(18)	O(32)-Mo(10)-O(58)	88.04(17)	O(37)-Mn(4)-O(39)	153.36(18)
O(26)-Mo(5)-Mo(8)	133.59(11)	O(58)-Mo(10)-Mo(3)	135.72(12)	O(37)-Mn(4)-O(53)	88.87(17)
O(26)-Mo(5)-O(56)	72.63(15)	O(58)-Mo(10)-O(4)	83.49(16)	O(37)-Mn(4)-O(15)	104.27(19)
O(54)-Mo(5)-Mo(8)	47.93(13)	O(58)-Mo(10)-O(22)	81.16(16)	O(37)-Mn(4)-O(65)	78.8(2)
O(54)-Mo(5)-O(14)	95.24(17)	O(3)-Mo(10)-Mo(3)	101.14(15)	O(39)-Mn(4)-O(53)	81.61(18)
O(54)-Mo(5)-O(26)	155.39(18)	O(3)-Mo(10)-O(4)	98.22(19)	O(39)-Mn(4)-O(15)	90.1(2)
O(54)-Mo(5)-O(56)	83.22(17)	O(3)-Mo(10)-O(22)	170.78(18)	O(39)-Mn(4)-O(65)	80.62(19)
O(54)-Mo(5)-O(7)	88.44(19)	O(3)-Mo(10)-O(24)	101.99(19)	O(53)-Mn(4)-O(65)	107.9(3)
O(56)-Mo(5)-Mo(8)	88.43(10)	O(3)-Mo(10)-O(32)	105.1(2)	O(15)-Mn(4)-O(53)	164.00(19)
O(7)-Mo(5)-Mo(8)	136.06(14)	O(3)-Mo(10)-O(58)	95.1(2)	O(15)-Mn(4)-O(65)	84.0(3)
O(7)-Mo(5)-O(26)	82.93(17)	O(10)-Mo(11)-Mo(1)	49.21(11)	O(6) ^{#1} -Mn(5)-O(8)	84.02(15)
O(7)-Mo(5)-O(56)	80.13(17)	O(10)-Mo(11)-O(26)	85.78(16)	O(6) ^{#1} -Mn(5)-O(10) ^{#1}	97.19(15)

O(29)-Mo(5)-Mo(8)	100.66(17)	O(10)-Mo(11)-O(48)	161.82(17)	O(6)#1-Mn(5)-O(12)	179.08(15)
O(29)-Mo(5)-O(14)	102.3(2)	O(10)-Mo(11)-O(56)	83.34(15)	O(6)#1-Mn(5)-O(14)#1	96.61(15)
O(29)-Mo(5)-O(26)	97.7(2)	O(26)-Mo(11)-Mo(1)	134.32(11)	O(6)#1-Mn(5)-O(24)	83.76(15)
O(29)-Mo(5)-O(54)	106.1(2)	O(26)-Mo(11)-O(56)	74.37(15)	O(8)-Mn(5)-O(10)#1	84.70(15)
O(29)-Mo(5)-O(56)	169.9(2)	O(42)-Mo(11)-Mo(1)	48.16(12)	O(8)-Mn(5)-O(14)#1	179.25(15)
O(29)-Mo(5)-O(7)	96.0(2)	O(42)-Mo(11)-O(10)	95.79(16)	O(8)-Mn(5)-O(24)	96.64(15)
O(8)-Mo(6)-Mo(2)	49.07(11)	O(42)-Mo(11)-O(26)	158.12(17)	O(12)-Mn(5)-O(8)	96.90(15)
O(8)-Mo(6)-O(18)	86.52(16)	O(42)-Mo(11)-O(48)	86.59(17)	O(12)-Mn(5)-O(10)#1	83.00(15)
O(8)-Mo(6)-O(30)	81.19(15)	O(42)-Mo(11)-O(56)	84.12(17)	O(12)-Mn(5)-O(14)#1	82.47(15)
O(8)-Mo(6)-O(43)	160.29(17)	O(48)-Mo(11)-Mo(1)	134.56(13)	O(12)-Mn(5)-O(24)	96.03(15)
O(18)-Mo(6)-Mo(2)	134.34(12)	O(48)-Mo(11)-O(26)	85.45(17)	O(14)#1-Mn(5)-O(10)#1	95.62(15)
O(18)-Mo(6)-O(30)	72.25(15)	O(48)-Mo(11)-O(56)	78.97(16)	O(14)#1-Mn(5)-O(24)	83.04(15)
O(30)-Mo(6)-Mo(2)	88.58(10)	O(56)-Mo(11)-Mo(1)	90.68(10)	O(24)-Mn(5)-O(10)#1	178.45(15)
O(64)-Mo(6)-Mo(2)	48.35(12)	O(62)-Mo(11)-Mo(1)	101.84(16)		
Symmetry	code:	#1, x+1, y,	z;	#2, -x+1, -y+1,	-z.

Table S4. Selected hydrogen bonding geometry (\AA , $^\circ$) for complex **1**.

D–H…A	D–H	H…A	D…A	D–H…A
N5–H5A…O60	0.86	1.97	2.807	163
N6–H6…O1	0.86	1.92	2.765	167
N8–H9…O33	0.86	1.91	2.766	173
N10–H10…O20	0.86	2.28	2.971	137

Table S5. The BVS calculation results of all the Mo atoms in complex **1**.

Atom	BVS
Mo1	5.210
Mo2	5.159
Mo3	5.232
Mo4	5.245
Mo5	5.254
Mo6	5.253
Mo7	5.258
Mo8	5.270
Mo9	5.200
Mo10	5.210
Mo11	5.210
Mo12	5.236

Table S6. Selection of catalyst dosage for diphenylmethane oxidation.

Entry ^a	Cat./mol%	Conv./%	Sel./%
1	0.18	36.2	>99
2	0.27	55.5	>99
3	0.36	69.3	>99
4	0.45	95.1	>99
5	0.55	91.4	>99
6	0.64	86.4	>99
7	0.73	79.3	>99

^a Reaction conditions: diphenylmethane (0.5 mmol), TBHP (2 mmol), phen (0.4 equiv.), MeCN (3 mL), 60°C, and 24 h.

Table S7. Selection of TBHP dosage for diphenylmethane oxidation.

Entry ^a	TBHP/mmol	Conv./%	Sel./%

1	0.5	28.2	>99
2	1	50.4	>99
3	1.5	73.8	>99
4	2	95.1	>99
5	2.5	95.3	98

^a Reaction conditions: diphenylmethane (0.5 mmol), complex **1** (0.45 mol%), phen (0.4 equiv.), MeCN (3 mL), 60 °C, and 24 h.

Table S8. Screening of oxidation temperature of diphenylmethane.

Entry ^a	Temperature /°C	Conv./%	Sel./%
1	75	86.4	98
2	60	95.1	>99
3	55	82.3	>99
4	50	70.1	>99
5	45	53.6	>99

^a Reaction conditions: diphenylmethane (0.5 mmol), complex **1** (0.45 mol%), phen (0.1 equiv.), TBHP (2 mmol), phen (0.4 equiv.), MeCN (3 mL), and 24 h.

Table S9. Screening of the amount of additive for diphenylmethane oxidation.

Entry ^a	Additive	Conv./%	Sel./%
1	—	5.3	>99
2	NaCl	35.5	>99
3	Na ₂ CO ₃	38.4	>99
4	NaHSO ₃	39.3	>99
5	Na ₂ SO ₄	41.7	>99
6	Na ₂ S ₂ O ₈	39.5	>99
7	Na ₂ SO ₃	45.7	>99
8	K ₃ PO ₄	29.2	>99
9	NaHCO ₃	24.2	>99
10	pyridine	53.9	>99
11	en	55.5	>99
12	TETA	48.4	>99
13	biz	38.1	>99
14	2,2-bpy	22.3	>99
15	imidazole	18.7	>99
16	phen	70.5	>99
17 ^b	phen	87.6	>99
18 ^c	phen	91.4	>99

19 ^d	phen	95.1	>99
^a Reaction conditions: diphenylmethane (0.5 mmol), TBHP (2 equiv.), catalyst (0.45 mol%), MeCN (3 mL), additive (0.1 equiv.) 60 °C, and 24 h; ^b phen (0.2 equiv.); ^c phen (0.3 equiv.); ^d phen (0.4 equiv.).			

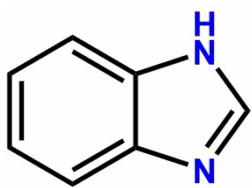
Table S10. Selection of solvents for diphenylmethane oxidation.

Entry ^a	Solvent	Conv./%	Sel./%
1	H ₂ O	—	—
2	MeOH	38.2	>99
3	EtOH	23.7	>99
4	MeCN	95.1	>99
5	AcOH	53.7	>99
6	DMF	63.2	>99
7	DMA	72.2	>99
8	dioxane	49.8	>99
9	isopropanol	51.8	>99
10	dichloromethane	40.2	>99

^a Reaction conditions: diphenylmethane (0.5 mmol), TBHP (2 mmol), catalyst (0.45 mol%), phen (0.4 equiv.), solvent (3 mL), 60 °C, and 24 h.

Table S11. Comparison of different catalysts for the oxidation of diphenylmethane.

Entry	Catalyst	t/h	T/°C	Conv./%	Sel./%	Ref.
1	Complex 1	24	60	95.1	>99	This work
2	[Co ^{III} (C ₂ N ₂ H ₈) ₃] ₂ [Co ^{III} (C ₂ N ₂ H ₈) ₂ (H ₂ O) ₂] _{0.5} [H _{2.5} PNb ₁₂ O ₄₀ V ^V V ^{IV} O ₂]	24	60	93.4	91.3	S6
3	[Pd(NH ₃) ₄] ₃ [V ₁₀ O ₂₈]	40	90	22.5	98.6	S7
4	[Cu ^I ₆ (trz) ₆ {PW ₁₂ O ₄₀ } ₂]	20	75	95.2	100	S8
5	{Zn[Cu(TCMOPP)]} · 2HN(CH ₃) ₂	20	80	37.1	>99	S9
6	[Cu ^I (4,4'-bipy)] ₃ [PMo ^{VI} ₁₀ Mo ^V ₂ O ₄₀ {Cu ^{II} (2,2'-bipy)}]	15	80	20.0	100	S10
7	{[Cd(DMF) ₂ Mn ^{III} (DMF) ₂ TPyP](PW ₁₂ O ₄₀)} · 2DMF	12	80	37.0	92.7	S11
8	[Co ₂ (L) _{0.5} (MTC)(μ ₃ -OH)(H ₂ O) ₂] · 2H ₂ O	15	90	95.6	>99	S12
9	Cu-BTC-SiO ₂	6	60	29.0	>99	S13
10	HKUST-1@Fe ₃ O ₄	14	80	94.7	95.2	S14
11	Co@GCNs-800	5	120	78.2	95.0	S15
12	[HFe ₄ O ₂ (H ₂ O) ₄ pydc] ₃ PW ₁₂ O ₄₀] · 10.5H ₂ O	24	100	95.7	96.6	S16
13	[Cu ^{II} ₄ Cu ^I (H ₂ trz) ₄ (C ₂ O ₄)(H ₂ O) ₄ (H ₃ PW _{11.18} Cu ^{II} _{0.82} O ₄₀)] · 8H ₂ O	6	75	93.0	>99	S17
14	Cu ^I ₁₂ Cl ₂ (trz) ₈ [HPW ₁₂ O ₄₀]	24	75	96.0	99.0	S18



Scheme S1. The ligand biz used in this work.

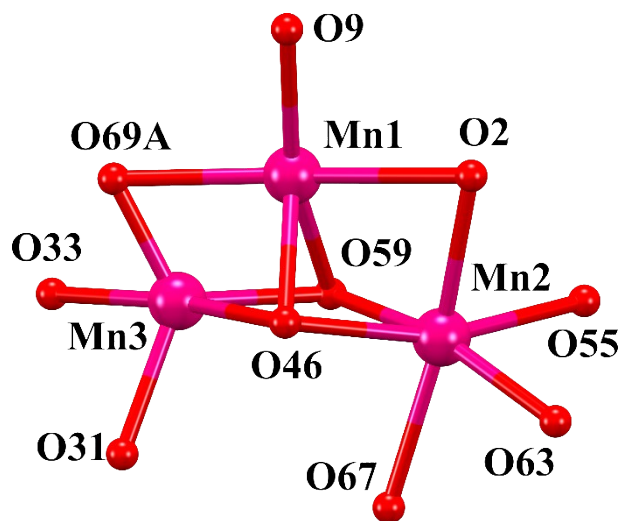


Fig. S1. The coordination environment of trinuclear manganese clusters in complex **1**. For clarity, all hydrogen atoms are omitted. O, red spheres; Mn, rose red spheres.

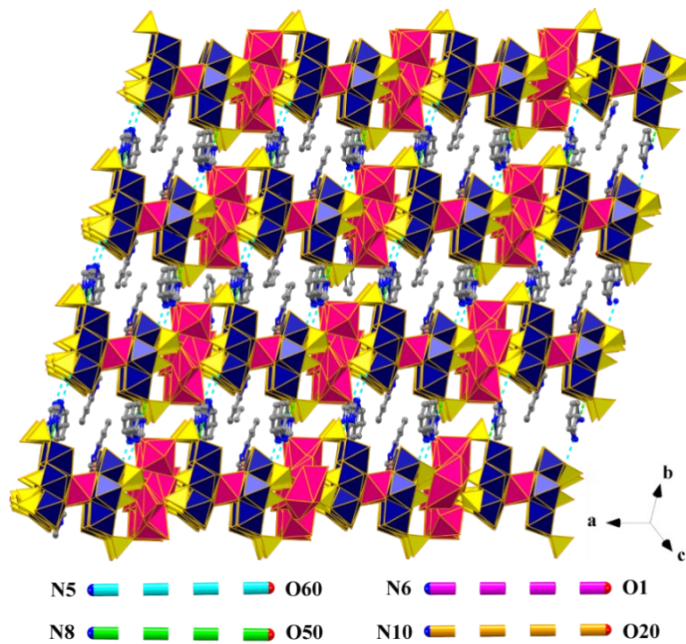


Fig. S2. Polyhedral view of the 3D supramolecular framework of complex **1**. For clarity, all hydrogen atoms are omitted. MoO_6 : dark blue octahedra; MnO_6 : rose red octahedra; PO_4 : yellow tetrahedra; C, gray spheres; N, blue spheres.

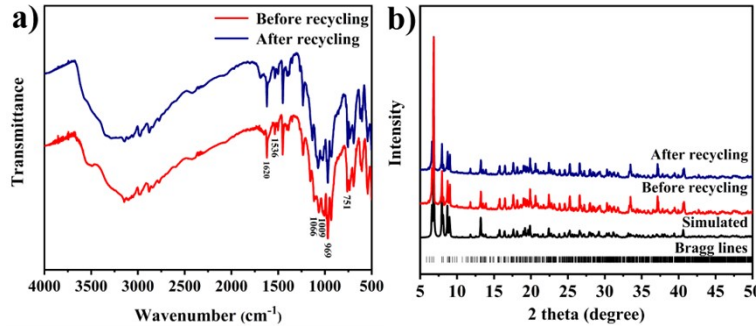


Fig. S3. a) IR and b) PXRD spectra of complex **1** before and after three runs of catalytic reactions.

The IR spectra of complex **1** exhibit the characteristic vibrations of the $\{\text{P}_4\text{Mo}_6\}$ polyanions: the peaks in the range from 1009 to 1066 cm^{-1} are attributed to the $\nu(\text{P}-\text{O})$ vibrations, the peak at 969 cm^{-1} is associated to $\nu(\text{Mo}-\text{O}_t)$, the peak at 751 cm^{-1} is assigned to $\nu(\text{Mo}-\text{O}-\text{Mo})$ vibrations. The weak absorption bands in the range of 1536–1620 cm^{-1} can be assigned to $\nu(\text{C}-\text{H})$ of the organic ligands, which further confirmed the components in the structure^{19,20}. The phase purity of complex **1** was determined by the good consistency between the experimental and simulated PXRD patterns and the predicted Bragg lines (Fig. S3b).

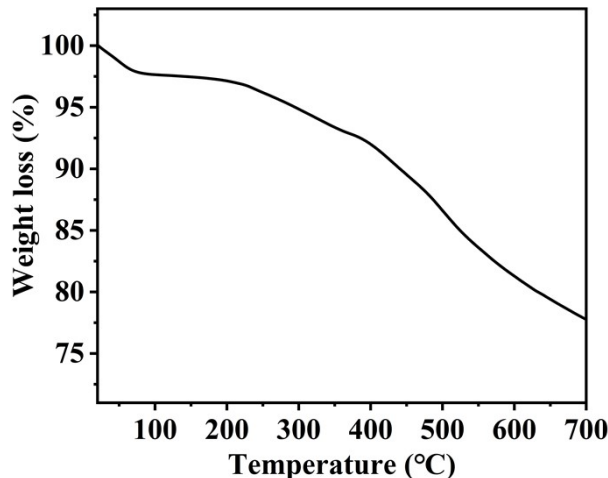


Fig. S4. The TG curve of complex **1.**

To explore the thermal stability of complex **1**, the TG measurement was carried out from 20 to 700 °C under a N_2 atmosphere at a heating rate of 10 °C min^{-1} . The TG curve suggests that complex **1** undergoes a two-step weight loss (Fig.S4). The first weight loss at 20–117 °C could be ascribed to the loss of all crystallization and physical adsorption of water molecules. The second weight loss from 117–700 °C is attributed to the thermal decomposition of organic ligands and polyoxometalates.

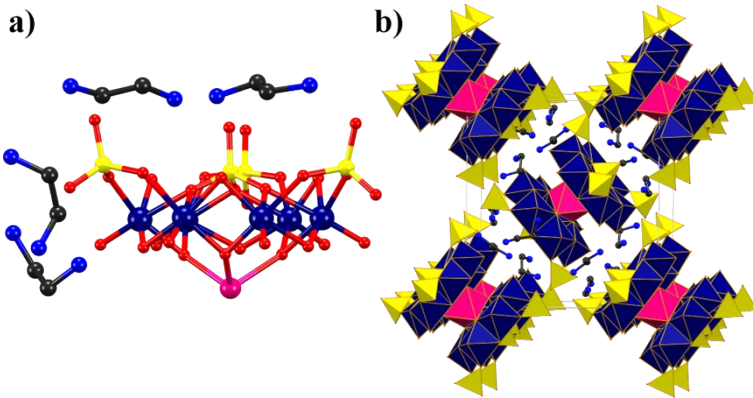


Fig. S5. a) The asymmetric unit of **NENU-607**. b) Three-dimensional polyhedron stacking of **NENU-607**. For clarity, all hydrogen atoms are omitted. MoO₆: dark blue octahedra; MnO₆: pink octahedra; PO₄: yellow tetrahedra; O, red spheres; C, black spheres; N, blue spheres; Mo, dark blue spheres; P, yellow spheres; Mn, pink spheres.

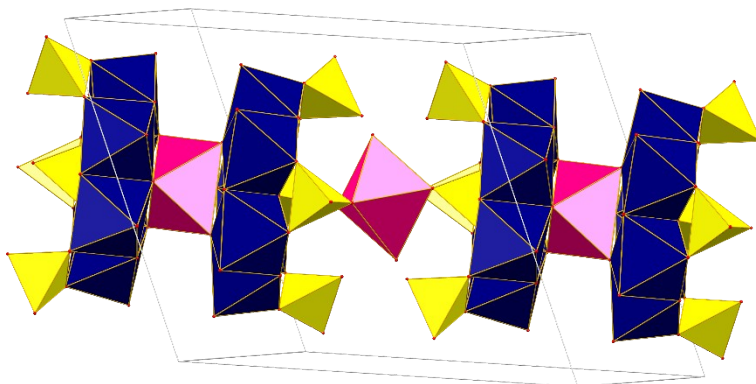


Fig. S6. Three-dimensional polyhedron stacking of **CUST-573**. For clarity, all hydrogen atoms are omitted. MoO₆: dark blue octahedra; MnO₆: pink octahedra; PO₄: yellow tetrahedra.

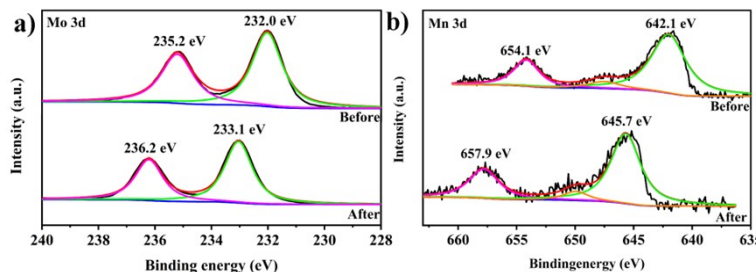


Fig. S7. The XPS spectra of complex **1** before and after reaction with TBHP.

Before the reaction of complex **1** with TBHP, the XPS spectra of Mo atoms show two peaks at 232.0 and 235.2 eV in the energy region of Mo 3d, which are typical Mo^V ion peaks. The XPS spectra of Mn atom exhibit two peaks at 642.1 and 654.1 eV in the energy region of Mn 3d, which are typical Mn^{II} ion peaks²¹⁻²⁴. After reacting with TBHP, two peaks at 233.1 and 236.2 eV appeared in the energy region of Mo 3d, indicating that Mo^V ions were oxidized to Mo^{VI} ions during the reaction. Two peaks at

645.7 and 657.9 eV appeared in the energy region of Mn 3d, indicating that Mn^{II} ions were oxidized to Mn^{III} ions during the reaction²¹⁻²⁴.

References

- S1. M. Sheldrick, *University of Göttingen*, 1990, **46**.
- S2. G. Sheldrick, *Acta Crystallographica Section A*, 2008, **64**, 112
- S3. Bruker AXS GmbH, SHELXTL v6.14, Bruker Analytical X-Ray Systems Inc., Madison, 2014
- S4. S. L. Xie, J. Liu, L. Z. Dong, S. L. Li, Y. Q. Lan and Z. M. Su, *Chem Sci.*, 2019, **10**, 185-190.
- S5. X. Wang, W. Mao, D. Wang, X. Hu, B. Liu and Z. Su, *Talanta*, 2023, **257**, 124270.
- S6. J. Hu, J. Dong, X. Huang, Y. Chi, Z. Lin, J. Li, S. Yang, H. Ma and C. Hu, *Dalton Trans.*, 2017, **46**, 8245-8251.
- S7. X. Huang, J. Li, G. Shen, N. Xin, Z. Lin, Y. Chi, J. Dou, D. Li and C. Hu, *Dalton Trans.*, 2018, **47**, 726-733.
- S8. D. Li, X. Ma, Q. Wang, P. Ma, J. Niu and J. Wang, *Inorg. Chem.*, 2019, **58**, 15832-15840.
- S9. Z. Zhang, X. Su, F. Yu and J. Li, *J Solid State Chem*, 2016, **238**, 53-59.
- S10. F. Farzaneh and F. Moghzi, *Reaction Kinetics, Mech. Catal.*, 2015, **115**, 175-185.
- S11. C. Zou, Z. Zhang, X. Xu, Q. Gong, J. Li and C. D. Wu, *J. Am. Chem. Soc.*, 2012, **134**, 87-90.
- S12. Y.-Y. Li, X.-H. Li, N. Xu, Z.-X. An, Y. Chu and X.-L. Wang, *Mol. Catal.*, 2023, **548**, 113428-113433.
- S13. G.-Q. Song, Y.-X. Lu, Q. Zhang, F. Wang, X.-K. Ma, X.-F. Huang and Z.-H. Zhang, *RSC Adv.*, 2014, **4**, 30221-30224.
- S14. L. Wang, J. Sun, X. Meng, W. Zhang, J. Zhang, S. Pan, Z. Shen and F. S. Xiao, *Chem. Commun.*, 2014, **50**, 2012-2014.
- S15. X. Lin, Z. Nie, L. Zhang, S. Mei, Y. Chen, B. Zhang, R. Zhu and Z. Liu, *Green Chem.*, 2017, **19**, 2164-2173.
- S16. Q. Wang, B. Xu, Y. Wang, H. Wang, X. Hu, P. Ma, J. Niu and J. Wang, *Inorg. Chem.*, 2021, **60**, 7753-7761.
- S17. Y. Wang, N. Xu, Y. Zhang, T. Zhang, Z. Zhang, X. H. Li and X. L. Wang, *Dalton Trans.*, 2022, **51**, 2331-2337.
- S18. B. Xu, Q. Xu, Q. Wang, Z. Liu, R. Zhao, D. Li, P. Ma, J. Wang and J. Niu, *Inorg. Chem.*, 2021, **60**, 4792-4799.
- S19. W. Wang, Z. Han, X. Wang, C. Zhao and H. Yu, *Inorg. Chem.*, 2016, **55**, 6435-6442.
- S20. S. Zhang, Y. Lu, X. W. Sun, Z. Li, T. Y. Dang, Z. Zhang, H. R. Tian and S. X. Liu, *Chem. Commun.*, 2020, **56**, 391-394.
- S21. J. Lin, N. Li, S. Yang, M. Jia, J. Liu, X. Li, L. An, Q. Tian, L. Dong and Y. Lan, *J. Am. Chem. Soc.*, 2020, **142**, 13982–13988
- S22. X. Li, C. Li, M. Hou, B. Zhu, W. Chen, C. Sun, Y. Yuan, W. Guan, C. Qin, K.

- Shao, X. Wang and Z. Su, *Nat. Commun.*, 2023, **14**, 5025
- S23. X. Jia, C. Streb and Y. Song, *Chem. Eur. J.*, 2019, **25**, 15548-15554
- S24. X. Fang, P. Kögerler, Y. Furukawa, M. Speldrich and M. Luban, *Angew. Chem. Int. Ed.*, 2011, **50**, 5212-5216